



NUMFRAC - a particle based code for fracture mechanics in non-linear materials

J.A. Åström^a

^aCSC - It-centre for science, P.O.Box 405, FIN-02101, Esbo, Finland

Abstract

NUMFRAC is a generic particle based code for simulation of non-linear mechanics in disordered solids. The generic theory of the code is outlined and examples are given by glacier calving and fretting. This text is a to a large degree a part of the publication: J. A. Åström, T. I. Riikilä, T. Tallinen, T. Zwinger, D. Benn, J. C. Moore, and J. Timonen, A particle based simulation model for glacier dynamics, *The Cryosphere Discuss*, 7, 921-941, 2013.

Project ID:

1. Elastic Model

NUMFRAC is a particle based code which has been designed to simulate fracture and fragmentation in non-linear, visco-elastic or plastic, materials. The code has previously been used for modelling, for example, brittle fragmentation [Åström, 2006], cytoskeleton dynamics [Åström et al, 2010], and mechanics of fiber networks [Åström et al, 2012]. A material is modelled as a set of elastic particles that are connected by non-linear interaction potentials. The code allows for arbitrary arranged 'packings' of particles of different size, kind and shape. For example, a rather loose random packing of spheres of different size and stiffness can be used as a model of an isotropic porous material with structure fluctuations. In contrast, a close packed hexagonal arrangement of identical spheres model a dense uniform anisotropic material. Geometry, interaction, and all other relevant parameters can be set separately for all particles and particle-particle interactions, making the code an excellent tool for investigating mechanical behaviour of strongly disordered materials.

To initialize a simulation, the particles are arranged and packed to form the desired material. Thereafter the connections are being determined and, for example, elastic beams, which then determines the potential, are set to connect some particles together.

The equations of motion may vary from case to case. A simple example is given by:

$$\mathbf{M}\ddot{\vec{r}}_i + \mathbf{C}\dot{\vec{r}}_i + \sum_j \mathbf{K}\vec{r}_{ij} = F_i, \quad (1)$$

where M is a mass-matrix containing the masses and moments of inertia of the particles, \vec{r}_i , $\dot{\vec{r}}_i$, $\ddot{\vec{r}}_i$ are the position, velocity and acceleration vectors of particle i , including rotations. \vec{r}_{ij} are the corresponding position vectors for all particles j that are connected to particle i . C is a damping matrices containing damping coefficient. K is the stiffness matrix and F_i is the sum of other forces acting on particle i . These forces may include gravitation, bouyancy, atmospheric and hydrodynamic/static forces, etc.

An example of an interaction potential between two particles is an Euler-Bernoulli beam. E-B beams can serve as an example of how interaction potentials are typically implemented. The elastic energy of a beam can be written as $(1/2)\mathbf{k}\vec{x}^2$, where \vec{x} is the displacement vector containing translational and rotational displacements of two connected mass points. If the components of the displacement vector, x_1 and x_4 are the displacements of the two connected mass points along the axis of the beam that connects them, x_2 and x_5 the displacements in the perpendicular direction and x_3 and x_6 the rotations of the mass points, the stiffness matrix \mathbf{k} for small deformations of a linear elastic Euler-Bernoulli beam in two dimensions is:

$$\mathbf{k} = \begin{pmatrix} \frac{EA}{L} & 0 & 0 & \frac{-EA}{L} & 0 & 0 \\ 0 & \frac{12EI}{L^3} & \frac{6EI}{L^2} & 0 & \frac{-12EI}{L^3} & \frac{6EI}{L^2} \\ 0 & \frac{6EI}{L^2} & \frac{4EI}{L} & 0 & \frac{-6EI}{L^2} & \frac{2EI}{L} \\ \frac{-EA}{L} & 0 & 0 & \frac{EA}{L} & 0 & 0 \\ 0 & \frac{-12EI}{L^3} & \frac{-6EI}{L^2} & 0 & \frac{12EI}{L^3} & \frac{-6EI}{L^2} \\ 0 & \frac{6EI}{L^2} & \frac{2EI}{L} & 0 & \frac{-6EI}{L^2} & \frac{4EI}{L} \end{pmatrix}, \quad (2)$$

where I is the moment of inertia of the beam cross-section, L the length of the beam, E Young's modulus and A the cross-section area of the beam.

In 3D the matrix must be extended to a size of 12×12 entries. Euler-Bernoulli beams overestimate the bending/shear stiffness for short and fat beams. That is, beams with an aspect ratio smaller than or roughly equal to 20. For smaller aspect ratios, Timoshenko beams may be used.

Another efficient and easy potential which we have also used for the ice application below, is to define a tension stiffness which is a harmonic potential with respect to the distance between two particles, and another harmonic potential with respect to node rotations away from the axis that connects the mid-points of the two particles. These two stiffness moduli can be directly linked to the macroscopic Young's modulus and Poisson ratio of the material to be modelled. This potential is a type of shear-beam.

Once the interactions for the particle-particle connections are determined and the appropriate stiffness matrices are assembled. The global stiffness matrix, \mathbf{K} , for the entire material body to be simulated is assembled by expanding, with zeros, the matrices for the individual particle-particle interaction matrices, and adding them together. Since the orientation is different for each interaction pair and the orientations change over time, the last term in Eq. 1 on the left side, is typically non-linear and can be obtained, for the present example, via:

$$\mathbf{K}\vec{r}_{ij} = T^T \int_0^t \mathbf{k}T dr_{ij}, \quad (3)$$

where dr_{ij} is the time dependent incremental displacement vector for connected particles i and j , T is a time dependent rotation matrix for converting a global coordinate system to the orientation of the beam axis connecting i and j .

In order to implement Eq. 1 on a computer, the differential equation must be rewritten as a difference equation via:

$$x(t + \Delta t) = \frac{\left[\frac{2\mathbf{M}}{\Delta t^2} - \mathbf{K}\right] x(t) - \left[\frac{\mathbf{M}}{\Delta t^2} - \frac{\mathbf{C}}{2\Delta t}\right] x(t - \Delta t)}{\left[\frac{\mathbf{M}}{\Delta t^2} + \frac{\mathbf{C}}{2\Delta t}\right]}, \quad (4)$$

where x is now the global position vector containing all particle translations and rotations. t is time and δt is the time incremental, i.e. time-step.

This discrete form is easily implemented on a computer and when, time and space-dependent, boundary conditions and $x(t = 0)$ is defined, the time development $x(t)$ can unambiguously be calculated.

For most fragmentation simulations there is further a need to determine a fracture criterion. If 'softening' potentials are used, like e.g. the Lennard-Jones potential, there is no such need since the attractive force between mass points vanish continuously. For harmonic potentials the fracture criterion must be defined explicitly.

Choosing a proper fracture criterion is far from trivial. A general elliptical criterion [Zhang and Eckert, 2005] that include the 'classical' fracture criterion of Tresca, von Mises, Mohr-Coulomb and the maximum normal, i.e. hydrostatic pressure, stress criterion is rather useful. This criterion states that a material under tension fails at locations where

$$\frac{\sigma^2}{\sigma_0^2} + \frac{\tau^2}{\tau_0^2} \geq 1, \quad (5)$$

in which σ is the normal stress, or pressure determined by the first invariant of the stress tensor and τ is shear stress determined by the second invariant. σ_0 and τ_0 are material dependent constant.

Because both shear and normal stresses are easily defined for beams it is straight forward to implement this fracture criterion in the beam model. A fracture limit can either be defined for every beam separately or as a limit on the average stress over several beams. For a single beam, σ can simply be set to the stress along the axis of the beam and shear τ the off-axis stress. For several beams (e.g. for all beams connected to a single mass point) the average stress tensor can be divided in a trace-less and a diagonal part which then defines local shear and normal stress, respectively.

2. Plastic and visco-elastic Models

In order for the particle model to be able to model not only fracture of elastic material, but also plastic and visco-elastic materials more elaborate interaction potentials, as compared to purely elastic ones, must be used. The microscopic mechanism behind plasticity and visco-elasticity is that local interactions can not just be broken but also reform in configurations different from the original one. This is the general principle behind irreversible material deformations like viscotic flow and plastic deformation. In the particle model, plasticity can be introduced via an ordinary yield/fracture stress criterion combined with an additional criterion that allow new contacts between particles to be formed. These new contacts may be formed between any two particles that come close enough to each other as the material deforms. With this mechanism, the material stress will not only be dependent on the load as in an elastic material before any fracture has taken place, but also on the load history.

A visco-elastic material differs from a plastic material in that the material stress depend not only on load and load history and also on time. This means that for, e.g. a constant, i.e. time independent, external load, stress will slowly relax to zero in a visco-elastic material.

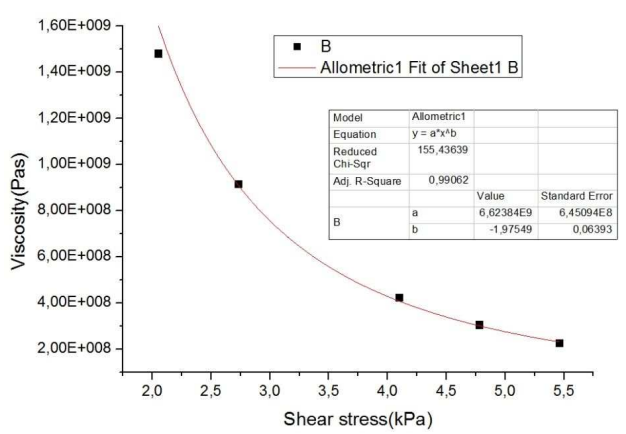


Fig. 1. A model test result for Glen’s flow law. A constant shear stress was applied to a model test square and strain rate was measured and viscosity extracted. The pre-factor A was set to roughly that of bitumen or asphalt, 10^9 . The simulation data, B , is represented by black squares and fitting the function, ax^b gave $a \approx 6 \times 10^9$, $b \approx 2.0$ as it should.

It is rather straight forward to incorporate these behaviours in particle models. To demonstrate the procedure, the incorporation of Glen’s flow law for ice rheology can be accomplished via, so called, “melting-freezing probabilities”. If these probabilities are set right, they can produce stress-dependent viscous flow obeying Glen’s law for flow rate, $\mathbf{D} = A(T)\sigma_e^{n-1}\mathbf{t}^{\mathbf{D}}$, where $A(T)$ is a temperature dependent Arrhenius factor, σ_e is the second invariant of the deviatoric stress tensor, \mathbf{D} is the strain-rate tensor, $\mathbf{t}^{\mathbf{D}}$ is the deviatoric stress tensor, and $n \approx 3$. In more quantitative terms, we assume that melting events are random and uncorrelated with induce a probability $P = 1 - e^{-\lambda\Delta t}$ for melting of a beam during a time interval Δt , where λ is the rate of melting. Each time a beam is broken, the elastic strain of that beam, which is proportional to $\xi = \sigma/E$, will be relaxed. Here ξ , σ and E are strain, stress and Young’s modulus of the beam. As long as the model material is under compression and the particles are close-packed, the model material will be practically incompressible. This implies that the flow rate of the simulated material will be a shear flow only and of the form $\mathbf{D} \approx \frac{\mathbf{t}^{\mathbf{D}}}{E}\lambda$. By choosing $\lambda = 2A\frac{U}{a^2}E^2 \approx A\sigma_e^2E$ we obtain Glen’s law $\mathbf{D} = A(T)\sigma_e^2\mathbf{t}^{\mathbf{D}}$. Here U is the elastic energy of the beam and a is the diameter of the discrete blocks (equals the spacing of the simulation lattice). Correspondingly, dynamic viscosity is $\mu = \frac{\mathbf{t}^{\mathbf{D}}}{\mathbf{D}} \approx \frac{E}{\lambda} \approx \frac{1}{A\sigma_e^2}$. A comparison of the model behaviour and Glen’s flow law is displayed in Fig. 1.

3. Application to fretting

Fretting is a usually harmful process that appear typically between metal parts during frictional wear of surfaces under compressive conditions. Fretting appear under strong enough compression for the frictional sliding to cause fracture of the metal surfaces. This is typically a problem for machine parts in e.g. engines. NUMFRAC can be used for simulating such surface wear. Here we tested the code by simulating a relatively fragile materials like e.g. a metal. The code produced the typical bent cracks and platelet formation observed in fretting [Kusner, 1982]. A microscopic picture from Ref. [Kusner, 1982] is displayed together with the corresponding simulation result in Figs 2 and 3. The crack shapes and platelet formation are, at least qualitatively, similar. In regard to this application the code is now ready to be adjusted to specific problems of industrial interest. Recently, also a three-dimensional version of fretting simulations have been developed.

One of the still unresolved problems for fretting simulations is that NUMFRAC is not able to simulate the very long lasting rapid oscillations that often lead to fretting damage in reality. Simulations are restricted to short times and a few oscillations only.

There are also other aspect of fretting, like time dependent viscosity and plasticity which all could be implemented but have not yet been done so. For realistic implementation, a close cooperation with experiments would be necessary.

4. Computational implementation

The codes has been constructed by the authors and do not use any commercial sub-routines or libraries. The codes are written in Fortran and use MPI for parallel computing. The scalability to large systems, i.e. many particles, is close to perfect. The origin of this scalability is the short range interaction of the particles combined with a domain decomposition algorithm. The code is optimized using standard techniques from molecular dynamics avoiding N^2 algorithm, where N is the number of particles. A clear majority, about 90%, of the computation time is spent in the force calculations. The most severe limiting factor is the time-step. There is no useful way in which time can be made parallel and, at present, the codes may, in the best case,

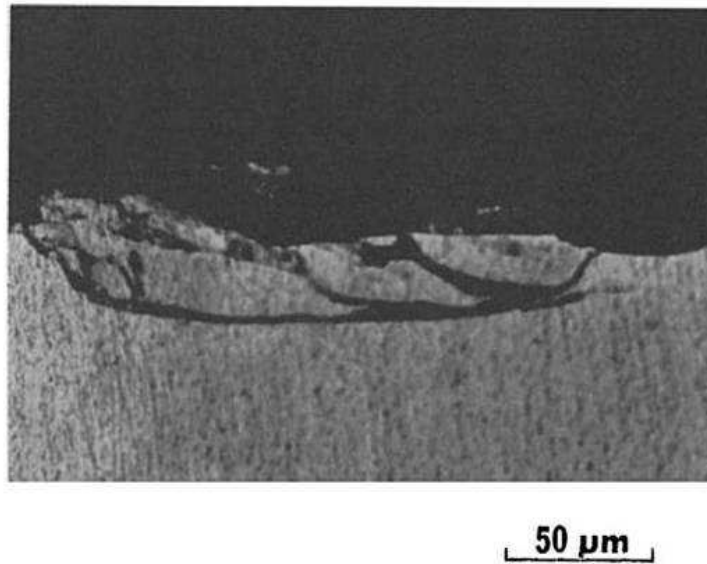


FIG. 8—A cross-sectional view, showing the subsurface crack growth and the formation of wear platelets. The geometric constraint prevented these particles from being removed. Test conditions: frequency, 100 Hz; load, 34.5 MPa; slip, 50 μm .

Fig. 2. Cross-section view of fretting damage platelets in magnesium. Picture from: D. Kusner et al, Materials Evaluation Under Fretting Conditions: A Symposium, American Society for Testing and Materials, 1982.

forexample, simulate about one hour of glacier dynamics in 24 hours of computing. The only reasonable way to speed up the computations is to use a viscosity that is considerably lower than that of ice as explained above. A typical fretting simulation takes about equally long. In this case the dynamics is very fast and the time steps needs to be reduced even further. A typical value is about 10^{-6} . Since computation of time cannot be made parallel, it is important, for computational efficiency to maximize the time-step without violating the stability of the computation. Since there are no explicit temperature fluctuations in the simulations and no connected heat-bath it is easy to check for stability by recording the total energy and check for energy conservation during simulations.

The particle size sets a very intuitive resolution limit for the simulation. At present the particles are of the order of one cubic meter, but the model is inherently scale invariant. As long as the equations of motion, Eq. 1 remain unchanged, all parameters can be re-scaled without changing the simulation results. This means, the same simulation can be view as a e.g. a cubic-meter or cubic-millimeter simulation if the length unit in r , \mathbf{M} , \mathbf{C} , \mathbf{K} and F are all changed accordingly. For example, if the length unity is decreased in a glacier simulation, \mathbf{M} and F , which is dominated by gravity, are reduced proportional to the volume of the particles, while \mathbf{K} is reduced only proportional to the surface area of the particles. This means that small glaciers are much more stable, under gravity, than large ones.

5. Scalability and PRACE

The NUMFRAC code has a two-dimensional version for which there is not much need for MPI-parallelisation. The major work within the PRACE effort to improve the NUMFRAC was the MPI-implementation in the three-dimensional version of the code. The main computational bottleneck of the 3D code is the very large number of particles needed for realistic simulation results (10^6 - 10^{10}) particles. The code is now designed so that the numbers of particles handled by each compute core remain, more or less, fixed. The total number, and thereby the system size, increases with the core number. Perfect scalability would thus be that the total compute-time / time-step would remain constant. Figure 4 demonstrates the scalability result for the NUMFRAC 3D code. The compute time for 100 time-steps is measured for various numbers of compute cores (Procs). The compute time increases slowly with system size indicating slightly less than perfect scaling. The tests were performed on the CSC CRAY XC30.

Acknowledgements

This work was financially supported by the PRACE project funded in part by the EUs 7th Framework Programme (FP7/2007-2013) under grant agreement no. RI-283493.

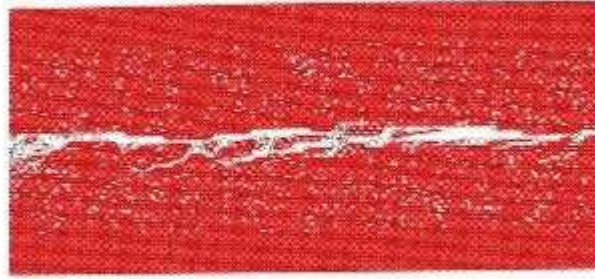


Fig. 3. NUMFRAC simulation of platelet formation

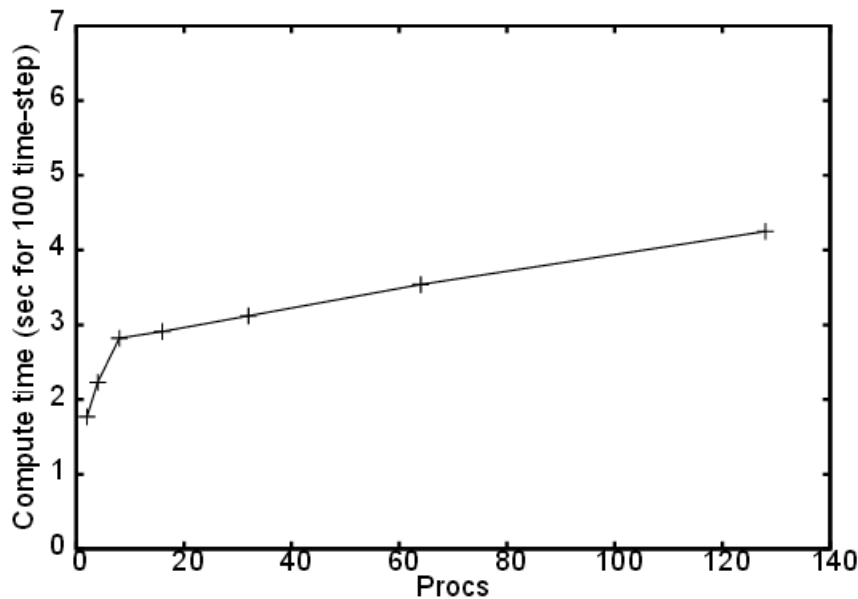


Fig. 4. Scalability of the NUMFRAC 3D code.

References

- Åström, 2006. Åström, J. A.: Statistical models of brittle fragmentation, *Adv. in Phys.*, 55, 247-278, 2006.
- Åström et al, 2010. Åström, J. A., von Althan, S., Sunil Kumar, P.B., and Karttunen, M.: Myosin motor mediated contraction is enough to produce cytokinesis in the absence of polymerisation, *Soft Matter*, 6, 5375, 2010.
- Åström et al, 2012. Åström, J. A., Sunil Kumar, P.B., and Karttunen, M.: Stiffness transition in anisotropic fiber nets, *Phys. Rev. E* 86, 021922, 2012
- Zhang and Eckert, 2005. Zhang, Z. F. and Eckert, J.: Unified Tensile Fracture Criterion, *Phys. Rev. Lett.* 94, 094301, 2005.
- Schulson, 1999. Schulson, E. M.: The Structure and Mechanical Behavior of Ice, *JOM*, 5 1, 21-27, 1999.
- Vaughan, 1995. Vaughan, D. G.: Tidal flexure at ice margins, *J. Geophys. Res.* 100, 6213, 1995.
- Kusner, 1982. D. Kusner et al, *Materials Evaluation Under Fretting Conditions: A Symposium*, American Society for Testing and Materials, 1982.